Aerothermal Analysis and Characterization of Shielded Fine Wire Thermocouple Probes

Laura Villafañe, Guillermo Paniagua

Turbomachinery and Propulsion Department
von Karman Institute for Fluid Dynamics
Chaussée de Waterloo 72
Rhode-Saint-Genèse, 1640, Belgium
Email: laura.villafane@vki.ac.b

Abstract

Thermocouple probes for high accuracy gas temperature measurements require specific designs optimized for the application of interest and precise characterization of the uncertainty. In the present investigation a numerical procedure is proposed that outperforms previous experimental approaches to analyze the thermocouple response and the different sources of temperature error. The results presented from conjugate heat transfer simulations on different shielded thermocouples provide information of the influence of the design parameters on the different error sources. These outcomes could help experimentalists to better design future instrumentation.

Keywords: thermocouples, conjugate heat transfer (CHT), recovery factor, conduction effects, response time, transfer function

1. Introduction

In transonic intake research [1] high fidelity in the total temperature is needed. In the present investigation numerical simulations were performed to study the steady and unsteady heat fluxes within a temperature probe to evaluate both the temperature during a transient and at equilibrium.

Multiple attempts to provide correction factors for standard thermocouple designs were found in the literature [2],[3],[4]. Traditionally over-all recovery factors were experimentally determined as an indicator of the temperature error of a thermocouple. Such global recovery factors accounted for the total effect of radiation, conduction and convection on the probe for a given flow environment. The variability of the heat fluxes balance within the probe with the environment and probe design, required each thermocouple to be carefully designed and calibrated for the required application. However, precise corrections from experimental probe calibrations are impractical. During such calibration not only the flow conditions need to be replicated but also the thermal interactions between the probe and the test bench. Furthermore, the precision to reproduce and to characterize the calibration environment determines the accuracy of the corrections.

The numerical characterization of the probes excelled previous experimental experiences in accuracy. The presented numerical methodology allowed understanding and quantifying the effects of the design parameters, required to achieve precise gas temperature measurements. Adiabatic recovery factors, conduction error estimations and response time characteristics were determined for a shielded probe with different values of thermocouple wire diameter, wire materials and boundary conditions at the thermocouple wire support. The presented numerical approach may be coupled with optimizers to design the best probe for any specific application.

2. Thermocouple Probe Design

2.1. Application

A transonic wind tunnel with a distorted annular sector, helicoidal test section was manufactured to study a novel heat exchanger [1]. Total flow temperature measurements were to be performed in this intermittent wind tunnel discharging to the atmosphere from a pressurized vessel. The flow temperature decreased during a test run

due to the flow expansion in the reservoir. Flow temperature traverses were to be recorded along the test section of about 0.013 m^2 transversal area. High-frequency response was required in order to allow fast traverses. A rake of temperature probes allowed to maximize the measurement locations in a test. Precise characterization of the probe response was necessary to synchronize all readings, as well as to accurately analyze the heat exchanger efficiency.

2.2. Pre-existent design rules

The temperature of a thermocouple junction is the result of the energy balances including the convective heat flux between the junction and the surrounding gas, radiation to the walls, and conductive flux to the wire. The balance is different for each probe and each condition. The measured temperature would be equal to the total flow gas temperature in the absence of radiative heat fluxes, conductive flux to the thermocouple support and dissipation of kinetic energy in the boundary layer.

General design rules provide advises to reduce the temperature error sources. A shield is recommended in order to decrease the error caused by the dissipation of kinetic energy in the boundary layer around the junction (often called velocity error). The shield also provides structural resistance in high velocity flows and reduces radiation effects. However decreasing the velocity of the flow decreases the convective heat transfer, penalizing the conduction error and the response time. Thus, the internal velocity must be kept as high as allowable. The internal velocity is function of the vent hole to inlet ratio. The junction position within the shield is a compromise between non-aligned entrance flow effects, and flow alteration due to convective heat transfer to the shield. Recommended values are given by Rom and Kronzon [3], Saravanamuttoo [5] and Glawe et al. [2]. The wires within the shield can be placed parallel or perpendicular to the flow. In the first case, the length of the wires is limited to prevent wire bending. In the second, the length is limited by the shield diameter.

Conduction errors can be estimated from the simplified solution of the 1D energy equation for a wire element dx, (Eq.1), considering symmetry boundary condition $\partial T/\partial x = 0$ at the junction ($x = 0$), and isothermal temperature $T_w = T_{sp}$ at the support of the wire ($x = l$). Eq. 2 provides a simplified solution particularized for the junction. The assumption of constant gas temperature and constant convection coefficient h, neglects the effect of the real flow temperature differences along the wire.

$$h(T - T_g)\pi d_w dx = k\frac{\partial^2 T}{\partial x^2}\pi\frac{d_w^2}{4}dx \tag{1}$$

$$T_{ad} - T_j = \frac{T_{ad} - T_{sp}}{\cosh(l\sqrt{\frac{4h}{k_w d_w}})} = \frac{T_{ad} - T_{sp}}{\cosh(l/l_c)} \tag{2}$$

Let us consider the total temperature of the gas T_g, equal to the junction recovery temperature T_{ad}, namely the total temperature in the absence of velocity error. Design rules derived from this simplified solution recommend to have high values of h (high velocities), high l/d_w ratios, low conductivity wire materials, and support temperatures close to gas temperature. Petit et al. [6] suggest that the ratio l/l_c should not be smaller than 5.

The contribution of the error due to radiation is generally important at high flow temperatures The simplified relationship (Eq.3) considering the most adverse conditions with unity view factor and equal conductive and radiative areas yielded a negligible error, lower than $4 \cdot 10^{-4}\%$, about 1 mK.

$$T_0 - T_j = \frac{K_R\sigma\epsilon A_R(T_j^4 - T_W^4)}{hA_c} \tag{3}$$

In flow temperature transients the energy balance at the thermocouple junction or on a dx at any position along the wire can be expressed by Eqs. 4. As in the steady case, T_g is considered equal to T_{ad} in the absence of velocity errors.

$$\begin{aligned} S_j h_j(T_g - T_j) + \frac{\pi}{2}d_w^2 k_w(\frac{\partial^2 T_w}{\partial x^2})|_{x=0} &= \rho_j C_{p,j} V_j \frac{\partial T_j}{\partial t} \\ h_w(T_g - T_w) + \frac{d_w}{4}k_w(\frac{\partial^2 T_w}{\partial x^2}) &= \rho_w C_{p,w}\frac{d_w}{4}\frac{\partial T_w}{\partial t} \end{aligned} \tag{4}$$

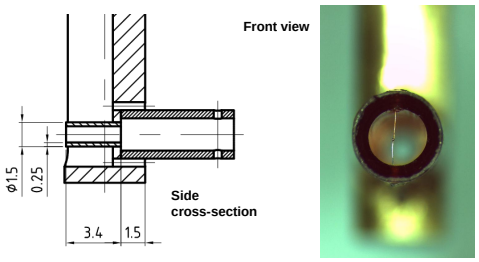

Figure 1: Shielded thermocouple probe.

In the case of uniform temperature on the junction, constant heat transfer coefficient independent with time, and no heat transfer by conduction between the junction and the adjacent wire, the thermocouple response to a temperature step is a first order system, Eq. 5. The assumption of first order system would be also valid for the assembly wire and junction if their diameters are identical, there are no radial or longitudinal temperature gradients, no conductive heat transfer to the supports, and the heat transfer coefficient is constant in time and along the length of the wire. Eq. 5, provides the time constant.

$$T_g = T_j + \tau \frac{\partial T_j}{\partial t}, \quad \text{with} \quad \tau_j = \frac{\rho_j C_{p_j} V_j}{h_j S_j}; \quad \tau_w = \frac{\rho_w C_{p_w} d_w^2}{4 k_g N u_w} \tag{5}$$

2.3. Shielded probe design

The temperature probe consists of a rake of five shielded thermocouples. Minimization of blockage effects given the small transversal area of the test section is considered, while preserving the structural resistivity of the whole rake. The geometric characteristics of the temperature probe heads are sketched in Fig. 1.

A type T thermocouple (copper-constantan) is placed perpendicular to the flow with a total length equal to the internal shield diameter, 2 mm. This wire configuration is intended to avoid wire bending at high velocities. Ratios $(l/d)_w$ of 79 are obtained with wires of 25.4 μ m diameter. The ratio weld-bead to wire diameter measured after probe manufacturing is about 2.7. The shield diameter is a compromise between the blockage minimization, wire structural resistivity and limitation of conduction errors. The shield is made of polycarbonate, chosen for its low conductivity. In agreement with the values recommended in the literature [2], [3], [5], the inlet/outlet area ratio is 4 and the junction is placed at 1/2 internal shield diameters from the entrance.

3. Methodology of the aerothermal study.

The transfer function of the thermocouple probe was numerically obtained by evaluating the response to a temperature step. Experimentally, the accuracy of the temperature corrections required a precise control of the gas temperature excitation and test conditions.

At the transonic conditions of interest, the characteristic time for the flow to develop around the thermocouple is two orders of magnitude smaller than the characteristic time of the thermal transient in the thermocouple wires. This allows performing simulations in two stages. First, a steady simulation is solved to establish the flow around the probe considered isothermal. The flow-field solution of this first step is imposed as initial condition for the simulation of the second step. In the second step, the solid boundary conditions are changed and a conjugate heat transfer (CHT) simulation is performed, solving the energy balances within the thermocouple. This second stage is ran in steady or transient state depending on whether the interest is focused on the steady temperature errors or on the transient behavior. In the latter case, the result is the response of the thermocouple to a temperature step. The decomposition in two stages highly reduces the computational cost.

This methodology allows the detailed analysis of the heat fluxes within the thermocouple probe, and the evaluation of the influence of the flow environment, probe geometry and wire materials.

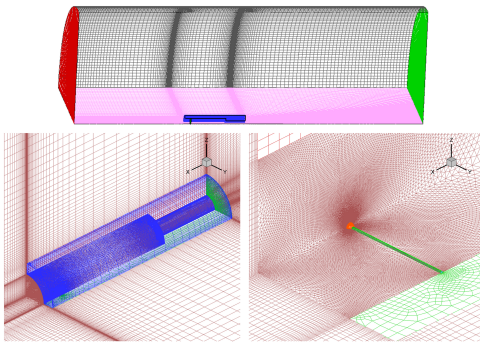

Figure 2: Computational domain. Left: TC shield view. Right: TC wire and junction.

Table 1: Probe geometric configurations.

	Geom 1	*Geom 2*	*Geom 3*
$l, [mm]$	1	1	1
$d_w, [mm]$	0.0254	0.0508	0
$d_j, [mm]$	0.07	0.14	0.07

4. Numerical Tools.

4.1. Computational domain and solver

The shielded thermocouple head is modeled in a 3D domain constituted by a quarter of a cylinder thanks to the existence of two symmetry planes on the probe geometry. The grid extends 6 shield diameters in the radial direction and in the axial direction upstream of the probe, and 10 diameters downstream. The three solid parts (shield, wire and junction) are meshed independently and concatenated to the gas domain mesh in the used NS solver. The gas hybrid 3D mesh composed by about 1.75 million cells is shown in Fig. 2-b. The grid is refined along the walls of the solid parts and specially around the thermocouple wire and junction (Fig. 2-c).

The Reynolds Averaged Navier Stokes solver employed was CFD++ (v.8.1). The k-epsilon turbulence model was considered. The initial values of k and epsilon were estimated in function of the free stream nominal velocity, with a free-stream turbulence level of 1% and a turbulence length scale based on the tube inner diameter. Values of y^+ in the vicinity of the thermocouple junction are lower than 0.3, and lower than 0.5 along the wire. For the steady simulations on both stages, convergence was achieved after 1000 iterations , 5.5 hours CPU time in 8 parallel Intel Core 2 Quad Q9400 (2.66 GHz) machines. For the transient CHT simulations the number of iterations required to achieved convergence varied depending on the wire material simulated. As an average 1000 iterations with different time steps were required, involving 51 hours CPU time running in 8 parallel machines. The integration time step was adjusted as function of the rate of evolution of the junction temperature, starting from 0.1ms.

4.2. Numerical test conditions

Nominal flow conditions for the simulations correspond to inlet boundary conditions $T_s = 273.22K$, $P_s = 101325Pa$, $V_\infty = 231.12m/s$, and $P_s = 101325Pa$ at the domain outlet. Different Mach and Reynolds numbers were tested for the geometrical configuration corresponding to the design geometry, Table**??**.

Three geometrical configurations were analyzed: *Geom 1,2 and 3*, (ref. 1). The shield is the same in the three cases. *Geom 1* corresponds to the design geometry. The modified parameter is the wire diameter, doubled in *Geom 2* where the ratio junction to wire diameter has been kept constant. *Geom 3* refers to the test case of a junction with infinitely thin wires.

Heat loss through the wires to the support is function of the wire dimensions and flow conditions (convection), but also of the material conductivity, and the support temperature. Different wire materials and boundary conditions at the support were analyzed for the configurations *Geom 1* and *Geom 2*. In all cases the shield material is polycarbonate and the junction properties are the average of the two materials of type T thermocouple. Other two materials of lower conductivity were considered: Nicrosil and an ideal material with conductivity equal to one, Tab. 2. The different support boundary conditions tested were:

(a) The shield-support behaves as an adiabatic solid,
(b) the shield is isothermal at 300 K,
(c) CHT on the shield.

Table 2: Material properties of thermocouple wires. Evaluated at 23°C.

	Copper	Constantan	Nicrosil	Ideal	Polycarbonate
K, [W m^{-1} K^{-1}]	401	19.5	13	1	0.2
ρ, [kg m^{-3}]	8930	8860	8530	8860	1210
C_p, [J kg^{-1} K^{-1}]	385	390	460	390	1250

5. Steady Temperature Effects

5.1. Global Temperature Correction

The junction temperature results from the balance between the convective heat fluxes gas-junction and gas-wire, and conductive flux junction-wire and wire-support. If those effects were decoupled, individual error equations could be used to estimate the deviation of the measured temperature. However, in practical applications the junction temperature must be evaluated by the simultaneous solution of the different heat flux rates [7].

The overall recovery factor Z (Eq. 6),the difference between the measured temperature (T_j) and the total gas temperature (T_0), can be decomposed into several contributions. The first term (a) is the velocity error, related to the adiabatic recovery factor. The second term (b), takes into account the temperature error due to conduction and convection along the wire, for a given support-shield temperature, (T_{sp}). The last term (c) collects the velocity error of the support-shield and the conduction effects between the shield, probe stem, and external probe support. The numerical method applied allows analyzing separately each contribution.

$$(1-Z) = \frac{T_0 - T_j}{T_0 - T_\infty} = \overbrace{\frac{T_0 - T_{ad}}{T_0 - T_\infty}}^{a} + \overbrace{\frac{T_{ad} - T_j}{T_{ad} - T_{sp}}}^{b} \cdot \overbrace{\frac{T_{ad} - T_{sp}}{T_0 - T_\infty}}^{c} \tag{6}$$

5.2. Velocity error

Temperature probes are intended to measure the gas total temperature, i.e. the temperature that the gas would attain if it is brought to rest through an isentropic process. However, in real gases frictional heat is generated within the boundary layer, hence the conversion of kinetic energy into thermal enthalpy is not perfect. The recovery factor, Eq. 7, represents the amount of kinetic energy recovered by the gas, where T_{ad} is the temperature of the surface of the junction if it would behave as an adiabatic body, and V is the reference upstream flow velocity. The recovery factor is function of the geometry of the immersed body and the Prandtl number of the fluid. Experimental values of adiabatic recovery factor determined by different authors [8],[9],[10] were presenteed by Moffat [11].

$$r = \frac{T_{ad} - T_s}{V^2/2C_p} = 1 - \frac{T_0 - T_{ad}}{V^2/2C_p} \tag{7}$$

For shielded thermocouples behaving as adiabatic bodies, the term (a) in Eq. 6 represents an overall adiabatic recovery factor, related to r by Eq.8. The velocity upstream of the junction within the shield(V) is different from the free stream flow velocity(V_∞).

$$Z_a = \frac{T_{ad} - T_s}{V_\infty^2/2C_p} = 1 - \frac{T_0 - T_{ad}}{V_\infty^2/2C_p} = 1 - (1-r)\frac{V_{int}^2}{V_\infty^2} \tag{8}$$

Experimental determination of recovery factors was impractical since the junction temperature has to be determined with great accuracy, and ensuring negligible influence of conduction to the supports, so the junction behaves as an adiabatic body. Steady simulations at different flow velocities allowed determining both r and Z_a and their sensibility to flow Mach and Reynolds numbers. Wire and shield were considered adiabatic solids in the computations and CHT was solved at the junction, at T_{ad}.

Computations were also performed considering all the solid boundaries adiabatic, junction included. The average temperature on the junction adiabatic surface $T_{ad,m}$ was compared with the junction temperature obtained when CHT was applied. Temperature differences were observed to be lower than 0.004 % ($T_{ad,m} - T_{ad}/T_{ad,m}$). These small differences were explained by the junction heat capacity.

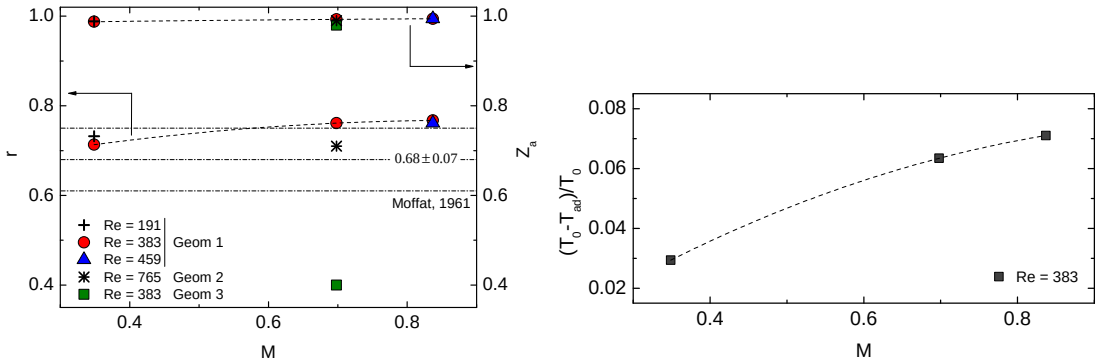

Figure 3: a) Recovery factors for different probe geometries, Mach and Reynolds numbers, b) Temperature error due to no isentropic flow deceleration

Figure 3(a) shows the evolution of the recovery factor (r), and the overall recovery factor (Z_a), for different Reynolds and Mach numbers. The adiabatic recovery factor slightly increases with the flow Mach number, and thus with the velocity within the shield (about six times slower than the external flow). The results are in good agreement with the recovery values compiled by Moffat [11]. For the same probe geometry *Geom 1*, at constant temperature and Mach number, an increase in the Reynolds number achieved through an increase in static pressure, results in a slightly decrease of the recovery factor. An increase of the Reynolds number at nominal flow conditions due to the increase of the wire and junction diameter *(Geom 2)*, yields to an analogous decrease of the recovery factor. The overall recovery factor shows the same trend but less sensitive to Mach and Reynolds variations.

Recovery factors were computed likewise for *Geom 3*, providing lower values. The flow behavior around a sphere is not similar to that around a thermocouple junction, neither to the flow parallel to a cylinder [11]. Comparison of the flow fields around the junction for *Geom 1* and *Geom 3*, showed a stronger flow deceleration in the first case forced by the presence of the wires, and hence, a thicker thermal boundary layer. Consequently the transformation of the flow kinetic energy into thermal energy is more efficient.

Although the recovery factor increases with the Mach number, the kinetic velocity rises in a higher amount, thus the temperature error represented in Fig. 3(b) also increases with velocity.

5.3. Conduction error

Free of velocity errors, the difference between the real junction temperature and the total temperature is the error due to conduction, namely the product of terms (b) and (c) in Eq.6. In a well designed thermocouple the junction temperature should be little sensitive to the support temperature, i.e. the term (b) is close to zero. In that case the overall contribution of conduction would be negligible whatever is the value of term (c). In real applications term (b) is different to zero.

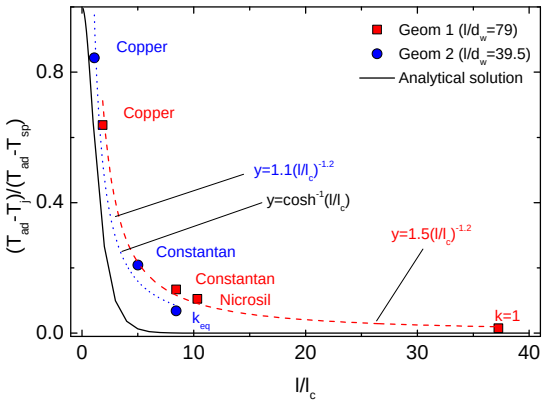

Figure 4: Ratio junction to support temperature deviations with respect to total temperature in function of the parameter l/l_c. Results from CHT simulations

Term (b) reflects the influence on the junction of the balance conduction-convection along the wire and the conduction with the support. Its contribution can be estimated by the solution of the one dimensional energy equation, Eq.2, that predicts an exponential decrease with the increase of the parameter l/l_c (for x$\geq$ 5, cosh x $\simeq$ 0.5e^x). Term (c) indicates the strength of the conduction heat transfer between the thermocouple and the support. The lower temperature of the shield-support with respect to the total gas temperature (T_{ad} in the absence of velocity error), $T_{ad}-T_{sp}$, drives the conduction to the wire. In the case the support would be perfectly isolated from external sources, it is function of the recovery factor of the complete shield/support. In real applications it is also function of the depth of immersion of the support in the flow, the support geometry and thermal properties, and the external boundary conditions of the probe.

The values of the parameter l/l_c for each material and the geometries *Geom 1 and 2* are indicated in Tab. 3. For the computation of l/l_c, Eq. 9, air conductivity is evaluated at the gas total temperature [7], and the Nusselt number is derived from a correlation for wires perpendicular to the flow [11]: $Nu = (0.44 \pm 0.06)Re^{0.5}$.

$$\frac{l}{l_c} = l\sqrt{\frac{4h}{k_w d_w}} = \frac{2l}{d_w}\sqrt{\frac{Nuk_g}{k_w}} \tag{9}$$

Table 3: Material parameters of thermocouple wires affecting conduction.

	Constantan	Copper	Nicrosil	Ideal	Equivalent
k, [kW m^{-1} K^{-1}]	19.5	401	13	1	6.89
l/l_c (Geom 1)	8.43	1.86	10.33	37.24	
l/l_c (Geom 2)	5.01	1.11	n.a.	n.a.	8.43

Fig. 4 shows the non-dimensional conduction temperature error corresponding to term(b) in Eq.6. All results correspond to complete CHT simulations. The temperatures difference ratio is plotted versus the parameter l/l_c, which for a given probe geometry is only varied by a change in the wire material. The error decreases as the parameter l/l_c increases indicating that the junction temperature is less influenced by the conduction effects. The results show two slightly distinct trends for each l/d_w case that are best fitted by power laws with a common exponent coefficient of -1.2. The equivalent material, k_{eq}, corresponds to an hypothetical material with a conductivity such that the l/l_c value for *Geom*2 is equal to the l/l_c value for constantan wire and *Geom*1 ($k_{eq} = k_{const}\sqrt{2}/4$). At this l/l_c value (8.43), the contribution of conduction of term (b) is slightly smaller for *Geom*2. The analytical prediction (Eq.2) underestimates the results when compared with the numerical results. This discrepancy can be explained by the simplifications introduced in the analytical solution, especially the assumption of homogeneous gas temperature and heat transfer coefficient along the wire, and equal to the conditions and geometry at the junction. The parameter l/l_c is a good estimator of the conduction error, but inappropriate to establish a unique relation

with the temperature error.

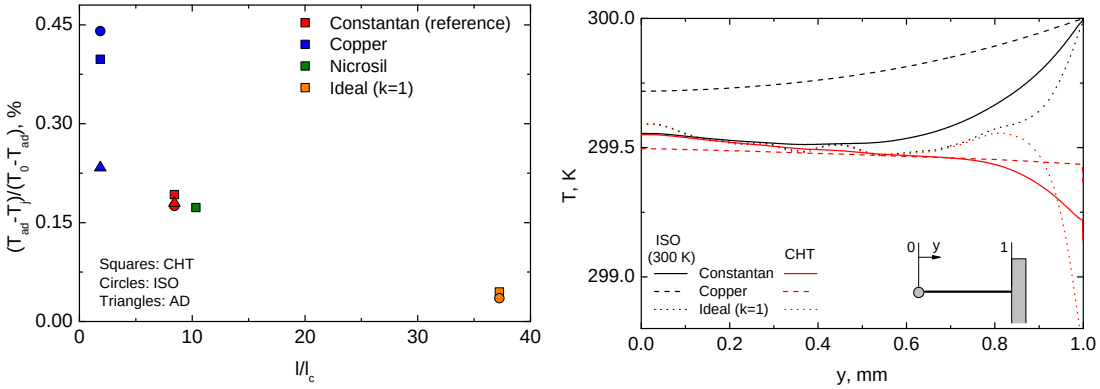

Figure 5: a)Overall temperature errors due to conduction in function of l/l_c, b)Wire temperature distributions

Figure 5(a) represents the global contribution to the conduction error computed for the reference probe geometry (*Geom*1) for different materials. The figure compares for a given wire material and geometry, thus a given l/l_c, the variability of the temperature error due to the conditions at the shield/support. Fig. 5(b) displays the temperature distribution along the wire in the same conditions for three of the materials and two of the boundary conditions, adiabatic support and CHT within wire and support. The junction temperature ($y = 0$) is the same for the ideal wire ($l/l_c = 37$) independently of the conduction at the shield, with an overall conduction error about 0.04 %. The temperature at each position along the wire is less affected by the longitudinal conduction, hence by the shield temperature, and more by the convective heat flux. Thus the temperature distribution is able to reflect the non homogeneity of the gas temperature around the wire. The junction is only influenced by the wire temperature adjacent to it, and the effect of the shield temperature penetrates until the last 20% of the wire. In the case of constantan wire the temperature along the wire is affected by conduction to the shield to a higher extent. However, the temperature at the junction converges to almost the same value for the different boundary conditions. Overall conduction errors vary between 0.18 and 0.19 %. In the copper wire case, with a l/l_c about 2, conduction with the support influences the junction temperature in a higher degree. Errors vary between 0.23 and 0.45% depending on the support conditions.

The reference adiabatic temperature considered for the analysis of the conduction errors is that of the junction. However, due to the strong flow deceleration taking place around the wire in the vicinity of the junction, there is a less efficient flow deceleration in this region. Thus, the temperature recovered is lower when compared to the junction. This effect can be observed in Fig. 5(b) for the ideal wire distribution in which the temperatures at 10 to 20 % from the junction are slightly lower than at the junction. It explains also the slight difference between the junction temperatures for constantan and ideal material wires. The higher conductivity of constantan forces the junction to stabilize at the lower temperature of the wire in the vicinity, while for the ideal material the temperature at the junction rises to almost the adiabatic temperature.

6. Transient Temperature Effects

The diffusion of the heat fluxes within the probe introduce a temperature lag on the junction temperature with respect to the gas temperature. The properties and geometry of the thermocouple wires affect the junction temperature evolution.

The numerical methodology applied in this study allowed analyzing the temperature evolution on the complete probe in response to a temperature step. All the results correspond to the nominal flow conditions, with an initial probe temperature equal to T_i=300 K.

The temporal evolution of the temperature along the constantan wire for *Geom*1 is displayed in Fig.6. At each position along the wires, the rate of temperature change is different. The response time of the shield is much

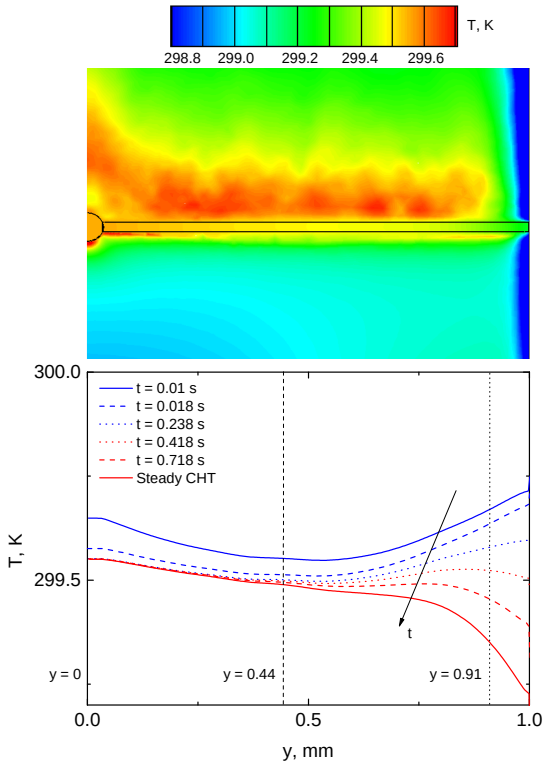

Figure 6: a)2D temperature contour, steady conditions. b) Evolution of constantan wire temperature distribution. CHT result

higher than that of the junction or wire due to its larger thermal inertia and lower thermal diffusivity a. Thus the part of the wire closer to the junction $y = 0$ reached the final temperature faster than the part of the wire close to the shield/support due to its influence by conduction. Figure 7 shows the time temperature history at three wire positions and a point within the shield, for constantan and copper materials. The temperature traces are made non dimensional with their steady value in order to compare the response times, not taking into account the differences on the final temperature achieved.

All the temperature distributions, except that of the shield, showed a fast initial temperature change, followed by a slower evolution. The fast initial temperature rise is dictated by the inertia of the junction or wire elements. The slow down is accentuated by the influence of the support at a certain position. In the constantan case the junction overpassed the conventional threshold of the 63.2 % of the response in 6.5 ms, and achieved the 90% of the final temperature in 18 ms. The temperature at $y = 0.44$mm showed a faster initial rise due to the lower thermal inertia of a wire element when compared with the junction, of bigger volume. However the convergence to the final temperature takes longer than in the junction due to the influence of the evolution of the shield at this point. The same behavior was observed at $y = 0.91$, but influenced in a higher degree by the shield temperature evolution.

The comparison of the temperature evolutions in the copper wire case, is analogous. When compared with the constantan results, the initial response of the copper is slightly slower, and the temperature evolutions at the different points closer in terms of the temperature rate evolution. It is explained by the higher conductivity of the copper, that implies higher diffusivity along the wire, and thus smoother temperature gradients between the different positions. Whereas in the constantan case, the effect of the support is little felt close to the junction but greatly affecting the opposite wire extreme.

In the ideal case of no existence of conductive heat between junction and wire, or if equal wire and junction diameters and no conduction flux with the support, the response of the thermocouple would be that of a first order system, Eq. 5. The characteristic would be the time required to complete 63.2 % of its response to a

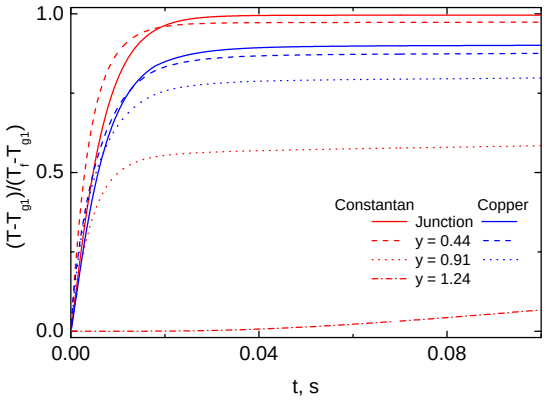

Figure 7: Temperature evolution at four control points on constantan and copper wires

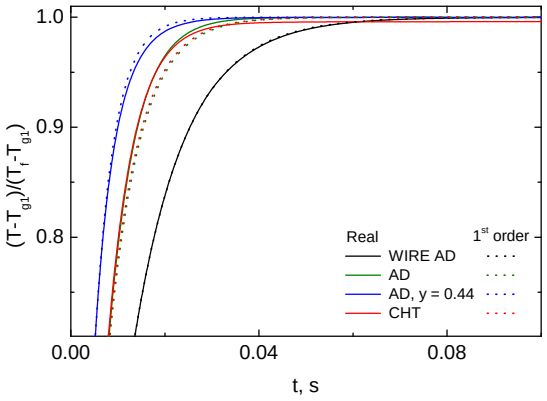

Figure 8: Comparison junction temporal evolutions with the correspondent first order.

gas temperature step. None of the wire temperature evolutions represented in Fig.7 corresponds to a first order response due to the influence of the support.

Non dimensional junction temperature evolutions are represented in Fig. 8 for the ideal case of adiabatic wire, and constantan wire with two different support conditions: CHT and adiabatic. For each evolution the time to reach 63.2% of the final temperature was used to evaluate the correspondent first order response. When the wires are considered adiabatic, the junction evolution collapses to the first order response. The presence of the wires modifies the temperature response whatever the condition at the support. When no flux occurs between shield and wires the junction reach the final temperature without the delay caused by the support but it does not correspond to a first order. This result is in agreement with the works of Yule [12] and Petit [6]. The influence of the wires causes an acceleration of the junction response if compared with the adiabatic wire result. It is instigated by conductive effects from the faster response of a wire element. The evolution at $y = 0.44$ is included in the graph for comparison. A simple decomposition in two first order systems expressing the response of the wire and support as done in cold wires [13] does not accurately reproduce the junction response in the presence of conductive effects.

Figure 9 displays the non dimensional junction temperature evolutions for different wire materials and the two wire diameters (*Geom*1 and *Geom*2). All cases correspond to complete CHT simulations with the consequent possible influence of the slower response of the support. For the cases in which the conductive effects on the junction are not too noticeable ($l/l_c \geq 5$), the higher the wire conductivity the faster the response of a wire element and therefore the faster the response of the junction. Increasing the wire and junction diameters introduces a delay in the response due to the increase of the thermal inertia, and a decrease of the parameter l/l_c, hence an increase

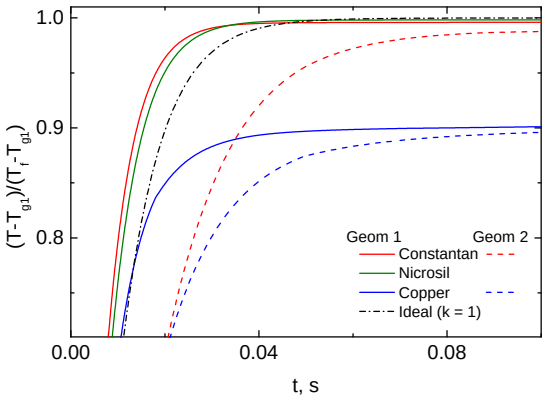

Figure 9: Junction temporal evolution. CHT simulations

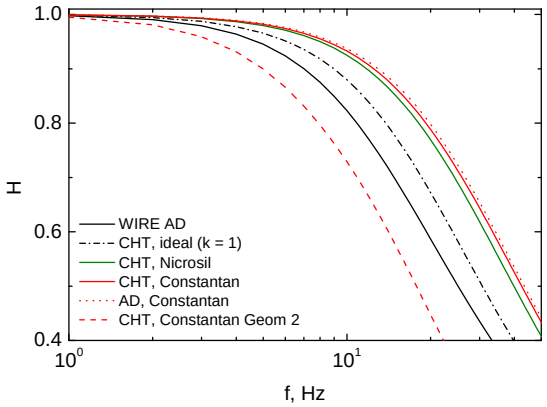

Figure 10: Transfer functions for different wire materials, wire diameter, and support conditions

of the conductive fluxes.

Assuming the response of a thermocouple can be expressed as linear system model of m-order, the transfer function of the thermocouple in the Z domain can be expressed by the ratio of two m-order polynomials, Eq. 10. A digital procedure [14] was used to determine the invariant transfer function that reproduces better the junction response in each case.

$$H(z) = \frac{b_0 \cdot z^{-d} + b_1 \cdot z^{-1-d} + \ldots + b_m \cdot z^{-m-d}}{1 + a_1 \cdot z^{-1} + a_2 \cdot z^{-2} + \ldots + a_m \cdot z^{-m}} \tag{10}$$

A first order response was found for *Geom*1 with adiabatic wires and for *Geom*3, in accordance with the temporal analyses. A second order system fitted the junction response when the support is adiabatic. A second order system represented likewise the complete CHT simulation in the case of the ideal wire material, where the conductive effects are negligible. For the case of the nicrosil wire, a third order response was found. The higher the effect of the support, the higher the order of the system found to represent the transfer function. The response was found to be that of a 5^{th} order system, for both *Geom*1 and *Geom*2 and constantan wire. For copper wires the response could be considered 5^{th} or 6^{th} order, although the fitting was less accurate. The transfer functions representing the junction responses for several test cases are shown in Fig. 10. The faster response corresponded to constantan wires with cutting frequencies slightly higher than 10 Hz.

7. Conclusions

A new methodology was proposed to numerically resolve the evolution of the heat transfer balances within a thermocouple probe. This procedure was applied to a shielded thin wire thermocouple, providing valuable information of the effect of the design parameters on the different error sources. This method overcame the experimental difficulties providing detailed information of the performances of a given probe in the range of flow conditions of interest.

Results from conjugate heat transfer simulations were analyzed at different values of the main non dimensional parameters driving the heat fluxes within the thermocouple probe. This approach allowed dissecting the commonly described experimental "recovery factor" into two steady error sources: flow velocity effects and conductive-convective errors. Radiation effects were shown to be negligible for the flow environment of interest.

Recovery factors for the shielded probe were computed at different Mach and Reynolds numbers. The temperature error increase due to velocity effects was evaluated, confirming the benefit of shield designs against bare thermocouples at high velocities.

Temperature errors due to conduction were analyzed for different test cases. The influence of conductive errors on the junction temperature is mainly dictated by the parameter l/l_c, which collects the effects of the wire conductivity, length and diameter and flow convective heat transfer, and by the support characteristics. The decrease of the temperature error with increasing values of l/l_c is reported. When values of the parameter l/l_c higher than 5 cannot be achieved, the junction temperature error is dominated by the wires support.

Time resolved CHT simulations allowed analyzing the temporal temperature evolution within the probe. The effect of the design parameters on temperature change rate was analyzed. The transfer function of the junction temperature response was obtained for the different tests simulated. The order of the lineal differential equation modeling the response was shown to increase with the influence of the conductive effects from the support on the junction. The response could be that of a second or third order differential linear system for l/l_c values higher than 10.

The presented methodology coupled with optimizers would provide a tool to design the best probe for a specific application.

Acknowledgments

This work was sponsored by TechSpace Aero in the frame of INTELLIGENT COOLING SYSTEM project. The financial support of the Region Wallone and the pole of competitiveness Skywin is acknowledged. The authors are grateful to V. Van der Haegen for his valuable contribution on the numerical work.

References

[1] L. V. ne, G. Paniagua, M. Kaya, D. Bajusz, S. Hiernaux, Development of a Transonic Wind Tunnel to investigate Engine Bypass Flow Heat Exchangers, Proc. IMechE, Part G: J. Aerospace Engineering 225, 8 (2011) 902–914.

[2] G. E. Glawe, R. Holanda, L. N. Krause, Recovery and Radiation Corrections and Time Constants of Several Sizes of Shielded and Unshielded Thermocouple Probes for Measuring Gas Temperature, Tech. rep., Lewis Research Center, Cleveland, Ohio (1978).

[3] J. Rom, Y. Kronzon, Small shielded thermocouple total temperature probes, Tech. rep., Institute of Technology, Israel (1967).

[4] T. M. Stickney, Recovery and time-response characteristics of six thermocouple probes in subsonic and supersonic flow, NACA TN 3455, Tech. rep., Lewis Flight Propulsion Laboratoty, Cleveland Ohio (1955).

[5] H. I. H. Saravanamuttoo, Recommended practices for measurement of gas path pressures and temperatures for performance assessment of aircraft turbine engines and components, Advisory Report 245, AGARD Advisory Report No. 245 (1990).

[6] C. Petit, P. Gajan, J. C. Lecordier, P. Paranthoen, Frequency response of fine wire thermocouple, J. Phys. E: Sci. Instrum 15 (1982) 760–764.

[7] M. D. Scadron, I. Warshawsky, Experimental determination of time constants and Nusselt numbers for bare wire thermocouples in high velocity air streams and analytic approximation of conduction and radiation errors. NACA TN 2599, Technical Note 2599, Lewis Flight Propulsion LAboratory, Cleveland, Ohio (1952).

[8] C. H. H, A. Kalitinsky, Temperature measurements in high velocity air streams, Trans. ASME 67 (1945) A–25.

[9] F. S. Simmons, Recovery Corrections for Butt Welded stright wire thermocouples in high velocity, high temperature gas streams, Tech. rep., NACA RM-E54G22a (1954).

[10] G. Glawe, F. S. Simmons, T. M. Stickney, Radiation and recovery corrections and time constants of several chromel-alumel thermocouple probes in high temperature high velocity gas streams, Tech. rep., NACA TN-3766 (1956).

[11] R. J. Moffat, Gas temperature measurement.

[12] A. J. Yule, D. S. Taylor, N. A. Chigier, Thermocouple Signal Processing and On-Line Digital Compensation, Journal of Energy 2, No 4 (1978) 223–231.
[13] R. Dnos, C. Sieverding, Assessment of the cold wire resistance thermometer for high speed turbomachinery applications, Journal of Turbomachinery 119, N0 1 (1997) 140–148.
[14] G. Paniagua, R. Dnos, Digital compensation of pressure sensors in the time domain, Experiments in Fluids 32, No 4 (2002) 417–424.